Polymer Chemistry

ROYAL SOCIETY OF CHEMISTRY

PAPER

View Article Online
View Journal | View Issue

Cite this: *Polym. Chem.*, 2021, **12**, 3619

Determining Michael acceptor reactivity from kinetic, mechanistic, and computational analysis for the base-catalyzed thiol-Michael reaction†

Sijia Huang,‡[a] Kangmin Kim, ‡[b] Grant M. Musgrave,[a] Marcus Sharp,[a] Jasmine Sinha, [a] Jeffrey W. Stansbury,[a,c,d] Charles B. Musgrave[a,b,c] and Christopher N. Bowman *[a,c]

Received 17th March 2021,
Accepted 26th May 2021

DOI: 10.1039/d1py00363a

rsc.li/polymers

A combined experimental and computational study of the reactivities of seven commonly used Michael acceptors paired with two thiols within the framework of photobase-catalyzed thiol-Michael reactions is reported. The rate coefficients of the propagation (k_P), reverse propagation (k_{-P}), chain-transfer (k_{CT}), and overall reaction ($k_{overall}$) were experimentally determined and compared with the well-accepted electrophilicity parameters of Mayr and Parr, and DFT-calculated energetics. Both Mayr's and Parr's electrophilicity parameters predict the reactivities of these structurally varying vinyl functional groups well, covering a range of overall reaction rate coefficients from 0.5 to 6.2 s^{-1}. To gain insight into the individual steps, the relative energies have been calculated using DFT for each of the stationary points along this step-growth reaction between ethanethiol and the seven alkenes. The free energies of the individual steps reveal the underlying factors that control the reaction barriers for propagation and chain transfer. Both the propagation and chain transfer steps are under kinetic control. These results serve as a useful guide for Michael acceptor selection to design and predict thiol-Michael-based materials with appropriate kinetic and material properties.

Introduction

Within the "click" paradigm, the thiol–vinyl reaction has attracted significant interest in synthetic organic chemistry, surface modification, polymer functionalization and in both linear and crosslinked polymer formation.[1] The thiol–vinyl reaction exhibits unique advantages such as rapid kinetics, minimal oxygen inhibition, negligible by-product formation, and nearly quantitative yield.[2–4] With these highly exploitable features, the thiol–vinyl reaction has been employed as a useful tool for dendrimer synthesis,[5] functional nanoparticle synthesis,[6] conjugation chemistry,[7,8] and bulk polymer synthesis.[9,10] The thiol-vinyl reaction family is mediated by various species such as radicals (*e.g.* thiol–ene reaction), bases, nucleophiles, and even highly polar solvents. The typical mechanism of radical mediated thiol–ene reactions involves the addition of a thiol across an alkene to produce a thioether. However, the radical intermediate can undergo homopolymerization steps with some vinyl species *via* a chain growth mechanism,[11,12] and hence leads to undesired side-reactions and network structures. Unlike the thiol–ene reaction, the base- or nucleophile-mediated reaction of thiols with a variety of electron-deficient alkenes, generally referred to as thiol-Michael reactions, proceeds only through a step-growth polymerization mechanism and yields minimal side products under appropriate conditions.

The thiol-Michael reaction proceeds either through a base-catalyzed pathway or a nucleophile-initiated pathway.[2] The major differences between those two reaction mechanisms relate to the types of proton sources and the reactive species that are attacked by the catalyst.[12] For the nucleophile-initiated thiol-Michael reaction, an electron deficient vinyl is commonly attacked by a phosphine-based nucleophile to form a strong basic enolate Zwitterion as the intermediate species. Subsequently, the potent enolate intermediate deprotonates

[a]*Department of Chemical and Biological Engineering, University of Colorado Boulder, 596 UCB, Boulder, CO 80309-0596, USA. E-mail: christopher.bowman@colorado.edu*
[b]*Department of Chemistry, University of Colorado Boulder, 596 UCB, Boulder, CO 80309-0596, USA*
[c]*Materials Science and Engineering Program, University of Colorado Boulder, Boulder, Colorado 80309, USA*
[d]*School of Dental Medicine, Craniofacial Biology, University of Colorado Denver, Aurora, Colorado 80045, USA*

†Electronic supplementary information (ESI) available. See DOI: 10.1039/d1py00363a

‡These both authors contributed comparably to this work.

the thiol species to yield the thiolate anion and an inert phosphonium ester. On the other hand, for the base-catalyzed pathway assessed here, the thiolate anion is directly generated by deprotonation *via* the base. In both pathways, the thiolate anion is responsible for the anionic cycle of the thiol-Michael reaction. However, the protonated base from the base-catalyzed pathway negatively impacts the reaction kinetics as an additional proton source, whereas the thiol species serves as the sole proton source for the nucleophile-initiated pathway. Therefore, the nucleophile-initiated thiol-Michael reaction, often using phosphines as catalysts, has the potential to proceed at higher reaction rates with lower catalytic loading relative to the base-catalyzed pathway. Chan *et al.* reported a detailed investigation of the monomer and organocatalyst effects on the nucleophile-initiated thiol-Michael reactions.[14] Due to the differences in the intermediate species for the nucleophile-initiated and base-catalyzed pathways, the kinetic parameters determined in previous studies are valid only for the nucleophile-initiated thiol-Michael reaction.

The base-catalyzed thiol-Michael approach has many of the same reaction features as the traditional nucleophile-initiated pathway, while facilitating temporal and spatial control of the reaction through recent advancements involving photobase-generators.[15–17] There are often no significant side reactions even when a large amount of base is used. Therefore, this work aimed to develop a fundamental understanding of the base-catalyzed thiol-Michael reaction, although a similar mechanistic approach could be developed and applied to the nucleophile-initiated thiol-Michael pathway. As such, the kinetic parameters and free energies calculated in this study are applicable only to the base-catalyzed pathway. The base-catalyzed thiol-Michael reaction involves a cyclic step-growth mechanism with alternating propagation (prop) and chain transfer (CT) steps (Scheme 1). The thiolate anion, deprotonated by a basic catalyst, adds to electron-deficient vinyl groups at the beta position, generating a carbanion intermediate (prop step). Depending on the stability of the intermediate carbanion, the carbanion may undergo a reverse reaction to reform the thiolate anion and vinyl reactants (*i.e.*, a reverse propagation step). Subsequently, this carbanion intermediate abstracts a labile proton from a free thiol to yield a thioether linkage and regenerate a thiolate anion (CT step), which subsequently initiates another prop step (Scheme 1).[13] Due to this step-growth nature of the thiol-Michael reaction, the overall reaction kinetics are controlled by both the prop and CT steps that alternate with each other. Therefore, a fundamental understanding of these individual steps enables the robust control of their kinetics, which has broad applicability for organic synthesis and materials design.[18]

It is well-established that the reaction kinetics and selectivity depend on the basicity of the thiol, basicity of the catalyst, electron deficiency of the vinyl group, and the solvent polarity.[13,19,20] The reaction kinetics of many common solvents,[19,21] bases,[20,22] and thiols[18,19] have been evaluated in both solution and bulk conditions. In all areas of implementation of the thiol-Michael reaction from small molecules to surface modification to polymer chemistry, a diverse range of Michael acceptors have been widely used and considered with little quantitative information available regarding their relative reaction kinetics, which ultimately plays a significant role in dictating the performance of the reaction in producing materials. The reaction kinetics and eventual selectivity of vinyl functional groups are inherently related to their structure and that of the rest of the molecule to which they are coupled, being well-described by the vinyl-specific propagation, reversed propagation, and chain transfer rate coefficients, k_P, k_{-P}, and k_{CT}, respectively. A recent study showed that in a ternary system of two vinyl compounds reacting with one thiol compound, the relative consumption rate and the selectivity of each vinyl compound was proportional to the differences in the k_p's of the vinyl functional groups.[23] While k_p provides considerable insight into the selectivity of vinyl compounds, the chain transfer rate coefficients (*i.e.*, k_{CT}) also play a central role in governing the overall reaction kinetics. Additionally, it has been reported that the anionic thiol-Michael reaction undergoes a reversible reaction at elevated temperatures.[24,25] Especially in a non-polar environment, the stability of the intermediate carbanion depends sensitively on the electron withdrawing nature of the vinyl structures. The intermediate carbanion can also undergo a reverse propagation step instead of a chain transfer step, depending on the free energy barriers. Consequently, the reverse propagation rate coefficient (k_{-P}) also provides another means for modulating the reaction

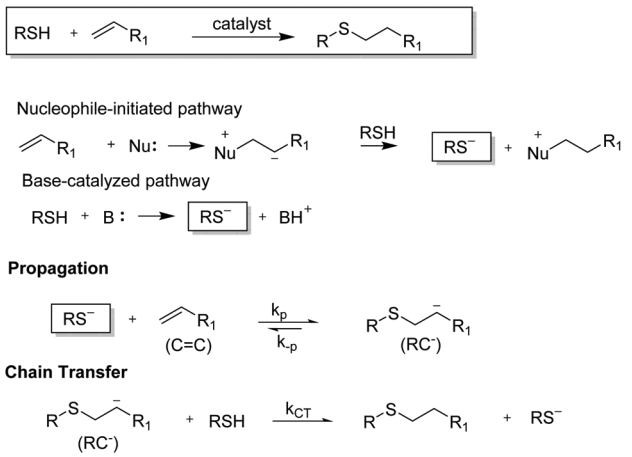

Scheme 1 The cyclic mechanism of the base-catalyzed and nucleophile-initiated thiol-Michael reactions between a thiol and an electron-deficient vinyl group[13]. A thiolate anion is generated by either initation pathway and then adds to the vinyl group, propagating with a rate coefficient, k_P. The resulting carbanion either undergoes a reverse propagation step with rate coefficient k_{-P}, or abstracts a proton from another thiol, transfering an active center with the rate coefficient, k_{CT}. Note that in the base-catalyzed pathway, a protonated base is formed during the initiation step, which as a protic species negatively impacts the reaction kinetics, whereas in the nucleophilic pathway the thiol compound is the sole proton source. Due to the different initiation steps and intermediate species, the rate coefficients and relative energies calculated in this study are applicable only to the base-catalyzed pathway.

characteristics and eventual properties of the thiol-Michael polymer network. As these results all suggest, a fundamental knowledge of the individual rate coefficients is essential for efficiently optimizing synthetic protocols that utilize thiol-Michael click reactions. In particular, a quantitative molecular structure – chemical reactivity relationship between the kinetic parameters and the vinyl structures enables the rational design and prediction of thiol-Michael reaction kinetics to produce specific polymer networks, new organic syntheses, and the identification and modification of biological targets.

The reactivity of vinyl compounds is frequently explained using the concept of electrophilicity.[26] Although this concept is commonly invoked, no single quantitative standard of electrophilicity exists to inform researchers. However, a few descriptive systems stand out because of their widespread use to predict the reactivity of various organic reactions. It has been demonstrated that the relative reactivity of structurally related electrophiles, *e.g.* with similar reaction patterns and degrees of steric hindrance, are successfully predicted by the LUMO energy of the electrophile.[27] Furthermore, as introduced by Parr, the global electrophilicity index (ω), defined as the square of the chemical potential divided by its chemical hardness, establishes an absolute scale of electrophilicity independent of the nucleophilic partner and the solvent environment.[28] This theoretical scale is often validated against the experimental scale developed by Mayr. As observed by Mayr and co-workers,[29,30] the rate constants for the reactions between nucleophiles and Michael acceptors are expressed by the experimentally derived correlation,

$$\log k = S_N(N + E),$$

where E is a nucleophile-independent electrophilicity parameter, N is an electrophile-independent nucleophilicity parameter, and S_N is an electrophile-independent nucleophile-specific susceptibility parameter. Among those electrophilicity parameters, Parr's ω and Mayr's E are the most widely used to predict the reactivity of electrophiles. For example, Parr's global parameters have been applied to predict the rate constants for Diels–Alder reactions,[31,32] nitrile oxide cycloadditions,[33] and catalytic oxidative cyanations of alkenes[26] while Mayr's electrophilicity parameters have been used to predict the absolute rate constants of 1,3-dipolar cycloadditions,[34] Darzen condensation of aliphatic ketones,[35] and targeted covalent inhibitors.[36]

A comprehensive reactivity scale of the electrophilicity (E) of Michael acceptors has been experimentally determined *via* a series of kinetic investigations confined to chemistries where nucleophilic attack of the Michael acceptors is the rate-determining step (RDS).[37] The electrophilicity parameter (E) was derived from the above equation and used to quantify the electrophilic reactivities of the Michael acceptors.[38] However, the crucial assumption in determining these parameters is that the nucleophilic attack is the RDS, which is not necessarily the case for many thiol-Michael reactions. For example, hexanethiol and maleimide are determined to have a k_p/k_{CT} ratio of 10 at ambient temperature, resulting in chain transfer-limited reaction rates. In these less typical yet frequently encountered cases, the electrophilicity resulting from these parameters may not explain some observations. Furthermore, k_{CT} itself cannot be acquired from these electrophilicity parameters without a fundamental understanding of the CT step. Consequently, it is not known whether these parameters contain the relevant information to determine the kinetic properties (k_P, k_{CT}, and k_{-P}) of thiol-Michael chemistries.

Herein, a systematic investigation is presented of the influence of structurally varied vinyl compounds on the individual kinetic properties of k_P, k_{CT}, and k_{-P} of thiol-Michael reactions involving two thiol compounds that proceed through chain transfer-dominated and propagation-dominated reactions with seven structurally dissimilar vinyl compounds with a wide range of electrophilicities. The rate coefficients were determined using real-time FTIR kinetic experiments, some of which correlate well with both Mayr's and Parr's electrophilicity parameters. Further, the thiol-Michael reactions between ethanethiol and the seven alkenes were modelled using DFT, which together with experimental results elucidate the mechanistic details of the prop and CT steps and add valuable insight into the thiol-Michael mechanism while providing the ability to accurately predict k_P, k_{CT}, and k_{-P} for these thiol-Michael reactions. This combined experimental and computational investigation exposes the limitations of the well-established electrophilicity parameters and extends the fundamental understanding of the molecular structure – chemical reactivity relationships between vinyl functionality and the reaction kinetics for these thiol-Michael reactions.

Results and discussion

Overall reaction rates

To evaluate the quantitative relationship of the kinetic parameters and the electrophilicities of the vinyl compounds, seven commonly used vinyl compounds with various electron deficiencies were chosen for the kinetic study (Fig. 1). For the thiol functional group, hexanethiol (HT) and butyl 3-mercaptopropionate (BMP) were chosen to study chain transfer-dominated reactions and propagation-dominated reactions, respectively. To minimize the polarity effect of the monomer and the viscosity change during reaction that affect the kinetics and thermodynamics, monofunctional reactants were chosen as model compounds for this study and all reactions were conducted in 2 M solutions of ethylene glycol diethyl ether (EGDE). Five vinyl compounds with previously reported electrophilicity parameters were experimentally examined in the reactions with HT and BMP in the presence of a photobase generator that releases the strong base tetramethyl guanidine (TMG) upon irradiation, with an initial 1 : 1 stoichiometric ratio of thiol: vinyl functional groups.

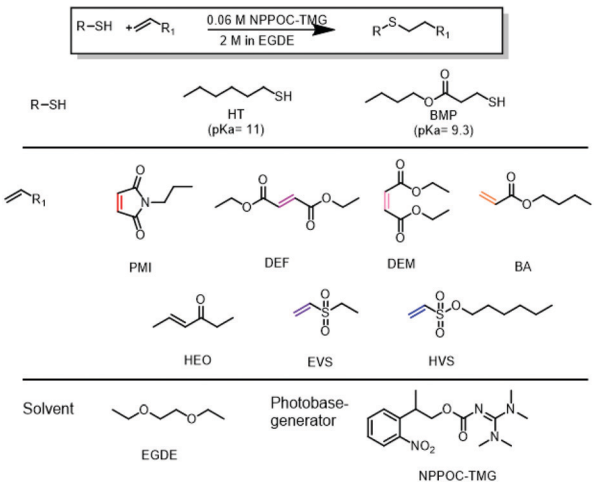

Fig. 1 Structure of the thiol, vinyl, solvent, and photobase generator used in this study.

The nearly complete consumption of both thiol and vinyl groups was achieved for all fourteen systems within 6 min of irradiation (Fig. S1–S14†). The consumption rate of the thiol functional group was similar to that of the vinyl group with an initial stoichiometric ratio of 1 : 1, indicating the absence of side reactions such as disulfide formation or homopolymerization within the cyclic mechanism. Vinyls with various functional groups were found to have significant differences in their reaction rates when reacting with HT under otherwise identical reaction conditions (in Fig. S1–S7†). For example, *N*-propylmaleimide (PMI) displayed the fastest reaction rate with both thiols while ethyl vinyl sulfone (EVS) and diethyl fumarate (DEF) exhibited faster reaction rates compared with diethyl maleate (DEM) and butyl acrylate (BA), which is consistent with previous observations.[1] It is noteworthy that the only difference between DEM and DEF is *cis vs.* trans isomerism with two identical ester electron withdrawing groups (EWGs), although DEF exhibits almost 4 times the reactivity of DEM when reacting with both thiols. To better understand the variation in the reactivity of those vinyl functional groups, the rate coefficients k_P, k_{CT}, and k_{-P} of each system were determined by using the least-squares method to fit the experimental kinetic plots to the kinetic model. Moreover, the calculated rate coefficients also predict the kinetic behavior in a network-forming polymerization system as shown in Fig. S15.† Hence, a detailed understanding of the individual kinetic steps is critical and a quantitative relationship between the rate coefficients and the electrophilicity parameters enables the rational selection and prediction of thiol-Michael reaction kinetics for both organic synthesis and polymerization design.

The reactivity of five vinyl compounds was experimentally determined and compared with both Mayr's and Parrs's global electrophilicity parameters as only the five vinyl compounds have available electrophilicity parameters from the literature.[36] In Fig. 3a and b, $k_{overall}$ is well-predicted with the electrophilicity parameters for the five vinyl compounds reacting with butyl 3-mercaptopropionate (BMP) (R^2 = 0.88 and 0.81). BMP with a pK_a of 9.8 is more acidic than hexanethiol (HT) with its pK_a of 11.[37] As a super base with a pK_a of 14, TMG is used to initiate the thiol-Michael reaction, and it is assumed that instantaneous deprotonation of the thiol is achieved regardless of their acidity due to the high basicity of the initiator and the maximal concentration of the thiol reactants. Therefore, the thiol pK_a difference has a negligible effect on the initiation step.

Once the thiolates that are initially generated by TMG react with vinyl groups, subsequent thiolate generation occurs in the CT step. With decreasing thiol concentration and the variability of the carbanion basicity due to different EWG's, the thiol pK_a difference increasingly affects the kinetics as the reaction proceeds. The more acidic thiol of BMP possesses a less basic conjugate thiolate with lower nucleophilicity than its HT counterpart. Similarly, the more acidic thiol of BMP is more readily deprotonated by the intermediate carbanion and tends to be more reactive in the chain transfer step. As a result, thiol-Michael reactions with BMP tend to be propagation-limited, which is confirmed by the experimental results (see ESI† Table 1 of rate coefficients for BMP). The correlations for the reactions with BMP confirm the initial claim that both Mayr's and Parr's electrophilicity parameters are predisposed to predict kinetic properties in the prop-limited system.

On the other hand, the more basic HT-based thiolate has a greater nucleophilicity than its BMP counterpart, and therefore, would be more likely to exhibit CT-limited reactions, which is not captured by Mayr's electrophilicity parameter based on its RDS assumption. Hence, for the reactions with HT, Mayr's parameters produce weaker correlations (R^2 = 0.62) with $k_{overall}$ as shown in Fig. 3c. Yet, both correlations demonstrate that the overall reaction rate increases with increasing electrophilicity of the vinyl components. However, neither Mayr's parameter nor Parr's electrophilicity parameter accurately predict the overall rate coefficients. As the understanding and prediction of individual steps is as critical as those of the overall reaction, the correlations of these parameters to the rate coefficients of the prop and CT steps were examined using DFT to further illuminate their governing principles. All free energies of the prop and CT steps for the base-catalyzed thiol-Michael reaction between ethanethiol and each of the vinyl compounds are summarized in Table 1 and reported in the potential energy surface plotted in Fig. 2.

Propagation step

In the previous section, the Michael reactions with HT were shown to be moderately correlated with both Mayr's and Parr's electrophilicity parameters, as these reactions tend to be CT-limited. Therefore, this work focused on these reactions to provide insights into their nature that are more subtle and less intuitive. In particular, the energetics associated with individual kinetic parameters were computed to develop a better understanding of the molecular structure – chemical reactivity relationship of the vinyl compounds and the reaction kinetics. The reactions kinetic parameters of these vinyls with BMP are available in the ESI Table S1.†

The first reaction within the cyclic mechanism is the prop step that is a nucleophilic attack by the thiolate anion on the

Table 1 Experimentally determined rate coefficients, corresponding Mayr's and Parr's electrophilicity parameters, and DFT-calculated energies for the seven vinyls considered in this study. The 95% confidence intervals of the rate coefficients are listed in parentheses

	$k_{overall}$ [a]	k_p [b]	k_{CT} [b]	k_{-p} [a]	Mayr's E	Parr's ω	$\Delta G^{\ddagger}_{prop}$ [c]	$\Delta G^{\ddagger}_{-prop}$ [c]	$\Delta G^{\ddagger}_{CT}$ [c]
PMI	6.2 (0.3)	30.0(1)	3.1 (0.4)	0.3 (0.1)	−14.1	2.6	8.8	7.1	6.3
DEF	4.3 (0.1)	8.0 (0.5)	5.3 (0.3)	13.0 (1.0)	−17.8	2.2	10.4	−0.3	4.6
EVS	3.4 (0.1)	3.0 (0.3)	11.0 (2.0)	3.0 (0.2)	−18.4	1.6	11.0	1.5	3.5
HEO	0.5 (0.05)	0.5 (0.1)	10.0 (2.0)	8.0 (0.6)	N/A	N/A	17.5	2.9	4.2
DEM	1.1 (0.1)	4.9 (0.5)	2.1 (0.6)	7.7 (0.9)	−19.5	1.7	8.6	1.4	6.2
BA	0.5 (0.04)	0.9 (0.1)	1.3 (0.2)	2.0 (0.3)	−19.6	1.5	17.0	4.4	6.5
HVS	2.5 (0.2)	4.4 (0.2)	1.2 (0.3)	0.6 (0.1)	N/A	N/A	9.4	6.4	7.2

[a] The unit of rate coefficients is s^{-1}. [b] The unit of rate coefficients is M^{-1} s^{-1}. [c] The unit of Gibbs free energies is kcal mol^{-1}.

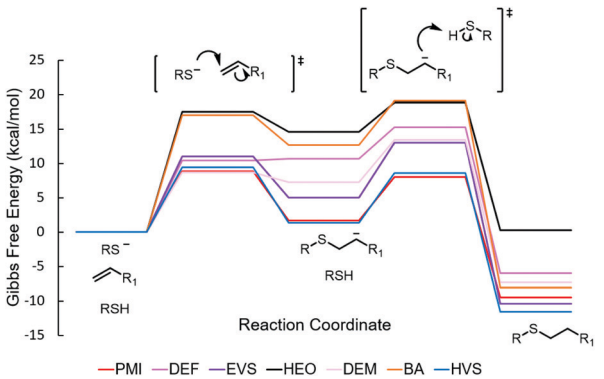

Fig. 2 Gibbs free energies of stationary points along the step-growth thiol-Michael reaction pathways for the reaction of ethane thiol and vinyl monomers. All vinyl compounds exhibit endergonic propagation reactions to generate the carbanion that subsequently abstracts a proton from a thiol in a stimulated environment using diethyl ether as the solvent. Chain transfer reactions are highly exergonic, driving the cyclic mechanism forward. The free energies are calculated by DFT at the MN15/6-31+g(d,p)/SMD-diethyl ether level of theory.

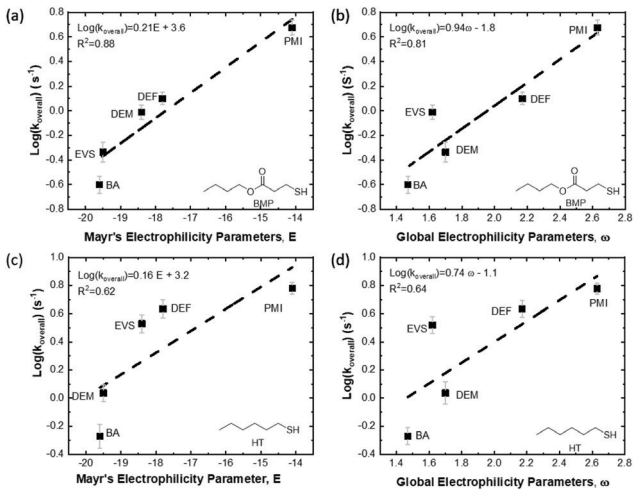

Fig. 3 Correlations between the overall rate coefficients and electrophilicity parameters for thiol-Michael reactions. Both Mayr's (a and c) and Parr's (b and d) electrophilicity parameters effectively capture the general reactivity trends with R^2 = 0.62–0.88 for the reactions between five vinyl compounds and two thiols. Note that the correlation is limited to only five vinyl compounds due to the sparce availability of electrophilicity parameters in the literature.

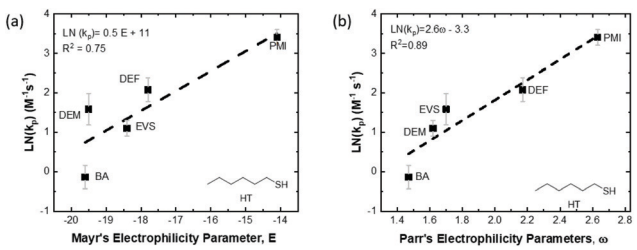

Fig. 4 Correlations between individual rate coefficients and Mayr's and Parr's electrophilicity parameters for thiol-Michael reactions with hexanethiol (HT). (a) Mayr's and (b) Parr's electrophilicity parameters are moderately correlated with the propagation rate coefficients (k_p) (R^2 = 0.75 and 0.89).

alkene functionalized with an EWG. Within such a nucleophilic reaction, the more electron-withdrawing substituents elicit greater reactivities in general. As Mayr's and Parr's parameters both focus on characterizing the electrophilic nature of the Michael acceptors, they should expectedly perform well in predicting the propagation rate coefficients of thiol-Michael reactions. Indeed, the evaluation of the propagation rate coefficients (k_P) confirms this hypothesis as Fig. 4a and b show that they effectively capture the general trend of the electrophilicity parameters (R^2 = 0.75 and 0.89) for the five vinyl functional groups considered. In particular, Parr's electrophilicity parameters show a good prediction of k_P (R^2 = 0.89). The linear regression is within the error range of the experimentally determined rate coefficients. To broaden further the fundamental insight into nucleophilic attack on the vinyl compound by thiolate anions (prop step), the computed energetics of seven vinyl compounds were calculated with a solvent model of diethyl ether and ethanethiol as a comparable proxy for hexanethiol. To optimize the computational costs and accuracy, the influence of alkyl length within the thiol-Michael reaction framework has been studied (see ESI 2.2† for a discussion of the influence of alkyl lengths on the energy). It was shown that ethanethiolate and hexanethiolate shows similar reaction free energies. Therefore, balancing between computational cost and accuracy, ethanethiolate was chosen for the computational energetic calculations. These seven vinyl compounds include *N*-propylmaleimide (PMI), diethyl maleate (DEM), diethyl

fumarate (DEF), 4-hexen-3-one (HEO), ethyl vinyl sulfone (EVS), butyl acrylate (BA), and hexyl vinyl sulfonate (HVS) and thus encompass a wide range of the types of vinyl compounds used in thiol-Michael reactions.

As expected, the activation energies of ethane thiolate reacting with the monovinyl compounds dictate the kinetics. With activation enthalpies ranging from −4.0 kcal mol^{-1} to 5.1 kcal mol^{-1}, these results broadly separate the seven monovinyl compounds into high and low reactive vinyls; HVS, PMI, DEF, and DEM are predicted to be more reactive than EVS, HEO, and BA, in agreement with our previously determined experimental propagation rate coefficients. Negative activation enthalpies occur in cases of strong attractive forces in transition states (TSs).[39] In these TSs the anionic charges of thiolates are significantly stabilized when a lone pair orbital of the attacking thiolate mixes with the π^* anti-bonding orbital of the vinyl compound. Because the activation enthalpies and activation free energies reflect the same reaction rates, entropic contributions are similar in these reactions according to Eyring's kinetic theory.[39] As hypothesized, the predicted entropic contributions to the free energy of activation of the vinyls do not significantly differ from each other at 25 °C with $-T\Delta S^{\ddagger}$ ranging from 11.6 kcal mol^{-1} to 12.9 kcal mol^{-1} (see ESI Table S2†) while predicted enthalpic activation barriers are strongly correlated with free energy barriers (R^2 = 0.97) (Fig. S21†). The negative entropic contribution (*i.e.*, positive $-T\Delta S$) results from the associative thiol-Michael reaction where two reactant molecules combine into one activated complex, which is therefore entropically disfavored because of its restriction of the rotational, vibrational, and translational degrees of freedom.[40]

When examining the carbanion intermediates that result from nucleophilic attack, the enthalpic reaction energies are uniformly exothermic ranging from −10.0 kcal mol^{-1} to −0.2 kcal mol^{-1}. The exothermic trend indicates that the thiolate anion is less stable than the resultant carbanion, as these energies are primarily related to the ability to stabilize the anionic charge *via* delocalizing electron density throughout the molecule. This ability is also closely related to the concept of electrophilicity that is broadly described by inductive (I) and resonance (M) effects. The inductive electron withdrawing effect (I^-) is prevalent in all of the molecules studied here, as atoms with higher electronegativities than hydrocarbons, namely oxygen, withdraw electron density *via* bond polarization. On the other hand, the resonance electron withdrawing effect (M^-) manifests itself only in molecules that exhibit a favorable orbital overlap between the p orbital of the carbanion and the π space of the electron withdrawing group,[41] where the orbital overlap is determined by structural compatibility. For example, DEF and DEM have identical ester functional groups on both sides of the vinyl bond, and thus equal inductive electron withdrawing effects. However, as a *cis*-isomer DEM does not have a geometry conducive to favorable orbital overlap from one ester through the vinyl grodup to the other ester, as a steric effect leads to a non-planar geometry with a ∼90° dihedral angle between the esters. On the other hand, DEF as a trans-isomer is planar, which enables favorable orbital overlap throughout the molecule (see ESI Fig. S19†). The interplay of various electron-withdrawing effects and molecular geometries leads to the superior kinetics of DEF over DEM. Such geometry-dependent electrophilicities are also observed in other examples. For instance, sulfonate-based HVS, despite having two sulfonyl π structures near the vinyl moiety, cannot distribute anionic charge through resonance as the anionic p orbital on the alpha carbon cannot effectively overlap with the tetrahedral centred structure. However, the inductive effects of the two sulfonate groups make them strong EWG's and render HVS highly electrophilic and reactive, in agreement with the experimental results.[42] In contrast, the maleimide-based PMI is exceptionally electrophilic due to its synergistic accumulation of inductive and resonance effects enabled by favorable orbital overlap.

Similar to the entropic trends in TSs, the entropic contributions to the reaction free energies of the prop step are similarly positive and lie in a narrow range from 11.1 to 13.5 kcal mol^{-1}. The endergonic trend of the prop step causes these reactions to occur through a late *TS*, where *TS* geometries more closely resemble the products than the reactants according to Hammond's postulate. Unsurprisingly, an analysis of the enthalpies of reaction and activation free energies for thiol-Michael prop steps shows that the Bell–Evans–Polanyi (BEP) relationship, which assumes a linear relationship between reaction energy and activation barrier (Fig. S20†), also holds relatively well. The BEP relationship was also demonstrated within the thiol-Michael framework in previous work on a ternary system.[23] When BMP was allowed to react with equimolar concentrations of EVS and BA in neat condition, the k_p of EVS was 14 M^{-1} s^{-1}, approximately twice that of the k_p of BA (6.4 M^{-1} s^{-1}). The final conversion of EVS was also ∼twice that of BA (65% *vs.* 35%). These trends agree with the expectation based on the BEP principle of a linear relationship between the kinetics and thermodynamics that results in the reaction being in the kinetic control regime.

Depending on the intermediate carbanion stability, some vinyl monomers show thermodynamically controlled propagation steps with small reverse barriers. Within these 7 vinyl monomers, the reverse propagation step's activation barrier ranges from −0.3 to 7.1 kcal mol^{-1}. DEF provides an example where the rate coefficient k_{-P} must be taken into consideration to understand its overall reactivity and kinetics. The reverse propagation barrier of DEF is only −0.3 kcal mol^{-1}, whereas the chain transfer energy barrier is 4.6 kcal mol^{-1}. Note that the negative free energy of the reverse propagation barrier (−0.3 kcal mol^{-1}) is within the error range of the computational calculation (0.5 kcal mol^{-1}). Therefore, only the trend of the energetics was focused on since the evaluated properties are beyond the resolution of the DFT method. The experimentally determined rate coefficient further corroborated this difference between the kinetic barriers. The reverse propagation rate coefficient, k_{-P}, is nearly two times higher than the chain transfer rate coefficient. The reverse propagation step has an important impact on the final conversion and the kine-

tics of intermediate species. Fig. 5 shows a kinetic model based on the calculated rate coefficients for functional group conversion *vs.* time for HT reacting with PMI and DEF, respectively. The k_P of PMI is 30 M^{-1} s^{-1} and the k_{-p} is 0.3 s^{-1}, whereas the k_P of DEF is 8 M^{-1} s^{-1} and k_{-p} is 13 s^{-1}. The final conversion approached 100% for HT and PMI. The thiolate (RS^-) and intermediate carbanion (RC^-) conversions continued to increase until plateauing at ~100 s. For DEF the reverse propagation reaction causes the final conversion to only reach ~95%. The thiolate concentration increases until reaching a plateau near 4%. In contrast, the concentration of the intermediate carbanion (RC^-) slightly increases in the first 60 s but then the reverse propagation reaction and chain transfer step drive the consumption of the intermediate carbanion.

This rapid reverse propagation step would slow the overall reaction rate significantly. However, the non-reversible CT step drives the reaction away from equilibrium and pulls it forward to make the mechanism overall energetically favorable. Hence, the reverse propagation step does not quench the thiol-Michael reaction. In general, a low reverse propagation barrier and less stable intermediate carbanion favor reversibility of the propagation step, whereas a high reverse propagation barrier and more stable carbanion disfavor the reverse propagation step. Finally, quantitative relationships between the energy barrier and the experimentally determined rate coefficients (k_p and k_{-P}) were determined with R^2 = 0.77 and 0.86, respectively, as shown in Fig. 6, providing insight that is missing in electrophilicity parameters.

Chain transfer step

Continuing in the cyclic mechanism of the thiol-Michael reaction, chain transfer occurs as the carbanion intermediate

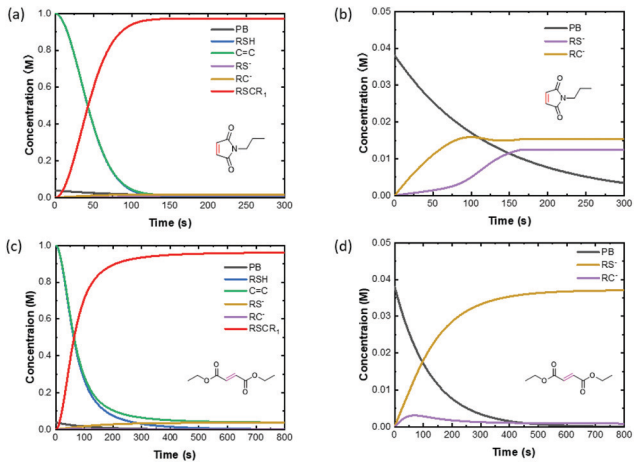

Fig. 5 (a) Kinetic model predictions for functional group conversion *vs.* time for the HT – PMI reaction; (b) Kinetic model predictions for thiolate and intermediate carbanion conversion *vs.* time for the HT – PMI reaction; (c) Kinetic model predictions for functional group conversion *vs.* time for the HT – DEF reaction and (d) Kinetic model prediction for thiolate and intermediate carbanion conversion *vs.* time for the HT – DEF reaction. All the kinetic model predictions are based on rate coefficients in Table 1 using MATLAB 2017b.

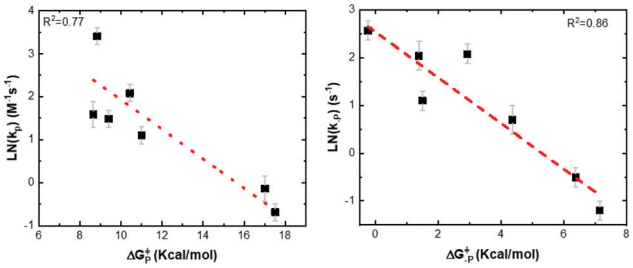

Fig. 6 (a) Correlations between propagation rate coefficients and activation energy barriers of the propagation step. (b) Correlations between reversed propagation rate coefficients and activation energy barriers of the reverse propagation step.

abstracts a proton from the thiol to form a thioether product while concurrently yielding another initiating thiolate. Chain transfer activation enthalpies for the seven vinyl compounds range from −9.8 to −4.8 kcal mol^{-1} while entropic contributions to the activation free energy ($-T\Delta S^{\ddagger}$) for CT range from 11.4 to 13.4 kcal mol^{-1}, which like propagation, renders the reaction enthalpically driven. Because the activation enthalpies for the CT step are more negative than those for the prop step, the activation free energies for the CT step tend to be smaller than those for the prop step, ranging from 1.6 kcal mol^{-1} to 7.2 kcal mol^{-1} (Table 1, Fig. 2). Having negative enthalpic barriers resulted in an even larger magnitude of negative reaction enthalpies ranging from −20 to −11.5 kcal mol^{-1}. Hence, the reactants composed of the intermediate carbanion and the thiol are much less stable than the final thioether adduct and new thiolate products. This, consequently, drives the reaction towards the final product. As thiolate was found to be less stable than carbanion, as discussed above, thiol must be less stable than thioether for this reaction to be exothermic. Therefore, under ambient conditions, a solution consisting of thiol and vinyl functional molecules is unstable and exhibits poor shelf stability even without addition of base species, especially for highly reactive vinyl compounds such as PMI and DEF. Additionally, such large exergonicities of CT reactions makes the reverse reaction highly unlikely and drives the polymerization forward by making the mechanism overall energetically favorable. Because the formation of the thiolate and thioether adduct does not result in a change in the number of reactant molecules of thiol and carbanion, the entropic contributions to the reaction free energy are only −0.6 to 2.1 kcal mol^{-1}, considerably smaller than the entropic changes of 10–13 kcal mol^{-1} for the prop steps. As a result, the CT thermodynamics are also mostly influenced by the enthalpy of reaction. It has been previously reported that the thiol-Michael reaction undergoes a reversible reaction for HEO and HT at 90 °C.[24] The polar solvent and elevated temperature would likely push the thermodynamic equilibrium to the reverse reaction. On the other hand, the reversibility with HEO is minimal in a less polar solvent and ambient temperature (25 °C). The kinetic analysis agrees with this hypothesis as the k_{CT} of HEO is 10 M^{-1} s^{-1} and k_{-CT} is 0.005 s^{-1}.

The common hypothesis that high electrophilicity leads to a faster prop and a slower CT step is further supported by the computational results. For example, HEO has a prop barrier of 17.5 kcal mol^{-1} and a CT barrier of 4.2 kcal mol^{-1} while HVS has a prop barrier of 9.4 kcal mol^{-1} and a CT barrier of 7.2 kcal mol^{-1}. This inverse energetic trend indicates that strong EWG's lead to a fast prop reaction but slow CT reaction. Again, when comparing the calculated free energy barriers with the experimental data, a general trend of the enthalpic barriers of CT and k_{CT} can be observed with R^2 = 0.93 (Fig. 7). The high coefficient of determination further confirmed that the CT step is mostly influenced by the enthalpy of the reaction. In contrast, no correlation exists between the enthalpic CT barriers and Mayr's *E*. The absence of a correlation with Mayr's *E* is expected because it is empirically determined with a set of kinetic data where the initial nucleophilic attack is the RDS and thus excludes information regarding subsequent reactions (*e.g.* CT step) (Fig. 8). As a result, neither Mayr's nor Parr's electrophilicity parameters display any predictive power regarding chain transfer reactions with R^2 = 0.19 and 0.34, respectively (Fig. 8a and b). The weak correlation is expected given the sole consideration of the prop step. Overall, the computational analysis of the prop and CT steps suggests that the electronic structures of the reactive species determine the enthalpies while changes in the number of species along the reaction coordinate primarily dictate the entropic contribution. Both the prop and CT steps tend to be kinetically controlled based on the computed free energy trends.

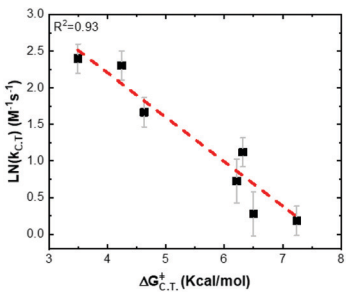

Fig. 7 Correlations between experimentally determined chain transfer rate coefficients and the computationally calculated activation energies of the chain transfer steps.

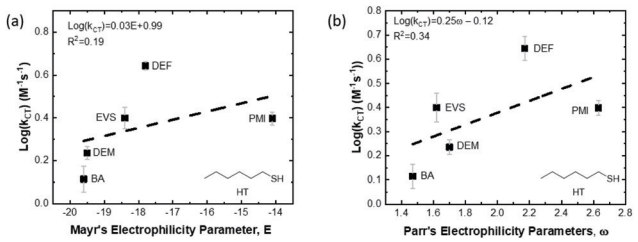

Fig. 8 Correlations between chain transfer rate coefficients and electrophilicity parameters for thiol-Michael reactions with hexanethiol (HT). Both Mayr's and Parr's electrophilicity parameters are poorly correlated with chain transfer rate coefficients (k_{CT}) with R^2 = 0.19 and 0.34, respectively.

Conclusions

In this contribution the effect of electrophilicity on vinyl compound reactivity within the framework of the thiol-Michael reaction was studied from kinetic and mechanistic perspectives. The kinetic behavior was examined for seven vinyl compounds and two thiols that have demonstrated a wide range of reactivities, including different RDS trends. Both Mayr's and Parr's electrophilicities were found to be correlated with the overall reaction rate coefficients for the reaction of five vinyl compounds with both thiols that exhibit propagation and chain transfer RDS's (R^2 = 0.62–0.88). These parameters are also correlated with k_P (R^2 = 0.75 and 0.89); however, they failed to demonstrate a relationship with k_{CT} (R^2 = 0.19 and 0.34). In order to gain insight into the individual steps, computational studies were conducted while expanding the scope to seven vinyls. All free energy activation barriers range from nearly barrierless to moderate (1.60 to 17.5 kcal mol^{-1}) for both prop and CT steps within the kinetically controlled reaction regime, explaining the rapid kinetics and click character of the thiol-Michael reactions. More specifically, both steps were found to be enthalpically driven, while the entropic penalty was much larger for propagation due to its associative nature in contrast to the metathesis-like nature of chain transfer. Electron withdrawing effects of functional groups were also examined in regard to orbital overlaps that determine the extent of resonance and inductive effects. The structurally similar *cis*/*trans* isomers with identical chemical formulas (DEF and DEM) display drastically different reactivities based on these orbital structures. This contribution examined the well-established electrophilicity parameters and exposed their limitations, elucidated the interplay between enthalpic and entropic effects on each reaction, and provided a fundamental understanding of the thiol-Michael reactions.

Experimental section

Materials

Butyl 3-mercaptopropionate (BMP), 1-hexanethiol (HT), ethyl vinyl sulfone (EVS), 1-butyl acrylate (BA), *N*-propylmaleimide (PMI), diethyl maleate (DEM), diethyl fumarate (DEF), 4-hexen-3-one (HEO), and ethylene glycol diethyl ether (EGDE) were purchased from Sigma-Aldrich. All monomers were used as received. The photobase generator (PBG) NPPOC-TMG and hexyl vinyl sulfonate (HVS) were synthesized according to previous literature.[42]

Real-time fourier transform infrared spectroscopy (FTIR)

All systems with three stoichiometric ratios *r* = 0.5, 1, and 2 of thiol:vinyl functional groups were reacted at ambient temperature. Reaction kinetics were monitored using a FTIR spectro-

meter (Nicolet 8700) at a rate of 2 scans per s. The sample was kept in an opaque bottle with an ice bath before characterization. Irradiation was performed using a mercury-lamp (Acticure 4000) with a 365 nm bandgap filter. The light intensity was maintained at 10 mW cm^{-2}, which was measured by an International Light. Inc. model IL 1400A radiometer. The thiol functional group (–SH) conversion was monitored by the reduction of the SH stretch peak located between 2550 and 2600 cm^{-1}, while the vinyl disappearance was monitored using the C=C stretch peak located at 810 cm^{-1} and 3100 cm^{-1} for acrylate and vinyl sulfone functional group. Three replicate experiments for each sample were performed.

Kinetic parameter determination

Based on the photobase-catalyzed thiol-Michael reaction kinetic, the species balances for the reactive moieties can be describe as

$$R_i = \frac{d[B]}{dt} = \frac{2.303 f \varepsilon I_0 \lambda}{N_{AV} hc}[PB] = k_i[PB] \quad (photoinitiation) \quad (1)$$

$$-\frac{d[C=C]}{dt} = k_p[C=C][RS^-] + k_{-p}[RC^-] \quad (propagation) \quad (2)$$

$$-\frac{d[RSH]}{dt} = R_i + k_{CT}[RC^-][RSH] \quad (chain\ transfer) \quad (3)$$

$$-\frac{d[RS^-]}{dt} = R_i - k_p[C=C][S^-] + k_{CT}[SH][RC^-] + k_{-p}[RC^-] \quad (4)$$

$$-\frac{d[RC^-]}{dt} = k_p[C=C][S^-] + k_{CT}[SH][RC^-] - k_{-p}[RC^-] \quad (5)$$

where f is the efficiency, $\in$ is the molar absorptivity of the NPPOC-TMG PBG, which has a value of 240 L mol^{-}·cm for 365 nm light;[21] [B] is the undegraded photobase concentration; I_0 is the light intensity; λ is the wavelength; N_{AV} is Avogadro's number; h is Planck's constant, c is the speed of light in vacuum, k_P is propagation rate coefficient, k_{-P} is reverse propagation rate coefficient, and k_{CT} is chain transfer rate coefficient. k_i was calculated from the slope of the photobase concentration *vs.* time plots for the first 300 s of reaction. (Fig. S16†)

For the simplicity of this work, the kinetic studies assumes: (a) the kinetic parameters k_{CT}, k_{-p}, and k_p remain constant throughout the reaction due to negligible diffusive and heat effects; and (b) the strong base catalyst leads to a nearly instantaneous deprotonation reaction. The rate coefficients of the propagation (k_P), reverse propagation (k_{-P}), and chain-transfer (k_{CT}) reactions were determined by using the lsqcurvefit solver in MATLAB 2017b to fit the experimental kinetic plots from 10% to 50% conversion, which was used to minimize any effects of inhibition or high conversion changes in the solvent, to the differential equations (eqn (1)–(5)). The overall reaction rate coefficient ($k_{overall}$) was calculated based on the slope of the kinetics plot from 10% to 50% conversion for a 1 : 1 stoichiometric mixture. The overall rate for a 1 : 1 stoichiometric mixture ([C=C]=[SH]) is expressed as $R_{overall} = k_{overall}[C=C] = k_{overall}[RSH]$.

Computational methods

The MN15 density functional[43] and 6-31+g(d,p) basis set were used throughout this study based on its accuracy (RMSE of 0.5 kcal mol^{-1} for reaction enthalpies and of 0.4 kcal mol^{-1} for free energies) relative to 12 functionals compared to the CBS-QB3 level of theory for computing the reaction energetics of elementary reactions involved in the thiol-Michael mechanism using *N*-methylmaleimide and methanethiol as the model chemistry (ESI 2.1.† Benchmarking of Computational Methods). Longer alkyl groups of hexanethiol used in experiments were truncated to an ethyl group after confirming an insignificant impact on the predicted energetics (ESI 2.2.† Influence of alkyl length on thiol-Michael reactions). All calculations were performed using the GAUSSIAN 16 (Revision A.03) software package.[44] Vibrational frequencies were computed to verify that the stationary states were optimized to the correct structures and to compute vibrational entropies, zero-point energies, and thermal corrections to enthalpies at 298 K. Solvent effects were described using the universal solvent model[45] with solvent parameters for diethyl ether because of its structural and dielectric similiarity to ethylene glycol diethyl ether used in experiments. Molecular structures were viewed using the Avogadro program.[46]

Conflicts of interest

There are no conflicts to declare.

Acknowledgements

We gratefully acknowledge financial support from the National Science Foundation (CHE 1808484), NIH/NIDCR R21DE028017 and the Industry/University Cooperative Research Center for the Fundamentals and Applications of Photopolymerization.

Notes and references

1 D. P. Nair, M. Podgórski, S. Chatani, T. Gong, W. Xi, C. R. Fenoli and C. N. Bowman, *Chem. Mater.*, 2014, **26**, 724–744.
2 C. E. Hoyle, A. B. Lowe and C. N. Bowman, *Chem. Soc. Rev.*, 2010, **39**, 1355.
3 H. C. Kolb, M. G. Finn and K. B. Sharpless, *Angew. Chem., Int. Ed.*, 2001, **40**, 2004–2021.
4 Y. Li, H. Su, X. Feng, Z. Wang, K. Guo, C. Wesdemiotis, Q. Fu, S. Z. D. Cheng and W.-B. Zhang, *Polym. Chem.*, 2014, **5**, 6151–6162.
5 S. Chatani, M. Podgórski, C. Wang and C. N. Bowman, *Macromolecules*, 2014, **47**, 4894–4900.
6 C. Wang, X. Zhang, M. Podgórski, W. Xi, P. Shah, J. Stansbury and C. N. Bowman, *Macromolecules*, 2015, **48**, 8461–8470.
7 Z. Liu, Q. Lin, Y. Sun, T. Liu, C. Bao, F. Li and L. Zhu, *Adv. Mater.*, 2014, **26**, 3912–3917.

8 V. S. Khire, T. Y. Lee and C. N. Bowman, *Macromolecules*, 2007, **40**, 5669–5677.
9 X. Zhang, S. Huang, M. Podgórski, X. Han, M. Claudino and C. N. Bowman, DOI: 10.1039/c8py00662h.
10 X. Zhang, W. Xi, S. Huang, K. Long and C. N. Bowman, *Macromolecules*, 2017, **50**, 5652–5660.
11 S. P. S. Koo, M. M. Stamenović, R. A. Prasath, A. J. Inglis, F. E. Du Prez, C. Barner–Kowollik, W. Van Camp and T. Junker, *J. Polym. Sci., Part A: Polym. Chem.*, 2010, **48**, 1699–1713.
12 P. Derboven, D. R. D'hooge, M. M. Stamenovic, P. Espeel, G. B. Marin, F. E. Du Prez and M. F. Reyniers, *Macromolecule*, 2013, **46**, 1732–1742.
13 S. Chatani, D. P. Nair and C. N. Bowman, *Polym. Chem.*, 2013, **4**, 1048–1055.
14 J. W. Chan, C. E. Hoyle, A. B. Lowe and M. Bowman, *Macromolecules*, 2010, **43**, 6381–6388.
15 K. Suyama and M. Shirai, *Prog. Polym. Sci.*, 2009, **34**, 194–209.
16 S. Matuszczak, J. F. Cameron, J. M. J. Fréchet and C. G. Wilson, *J. Mater. Chem.*, 1991, **1**, 1045–1050.
17 C. O. Hayes, W. K. Bell, B. R. Cassidy and C. G. Willson, *J. Org. Chem.*, 2015, **80**, 7530–7535.
18 N. J. Darling, Y. S. Hung, S. Sharma and T. Segura, *Biomaterials*, 2016, **101**, 199–206.
19 B. H. Northrop, S. H. Frayne and U. Choudhary, *Polym. Chem.*, 2015, **6**, 3415–3430.
20 S. H. Frayne, R. R. Murthy and B. H. Northrop, *J. Org. Chem.*, 2017, **82**, 7946–7956.
21 G. B. Desmet, M. K. Sabbe, D. R. D'hooge, P. Espeel, S. Celasun, G. B. Marin, F. E. Du Prez and M.-F. Reyniers, *Polym. Chem.*, 2017, **8**, 1341–1352.
22 W. Xi, H. Peng, A. Aguirre-Soto, C. J. Kloxin, J. W. Stansbury and C. N. Bowman, *Macromolecules*, 2014, **47**, 6159–6165.
23 S. Huang, J. Sinha, M. Podgórski, X. Zhang, M. Claudino and C. N. Bowman, *Macromolecules*, 2018, **51**, 5979–5988.
24 B. Zhang, Z. A. Digby, J. A. Flum, P. Chakma, J. M. Saul, J. L. Sparks and D. Konkolewicz, *Macromolecules*, 2016, **49**, 6871–6878.
25 P. Chakma, L. H. R. Possarle, Z. A. Digby, B. Zhang, J. L. Sparks and D. Konkolewicz, *Polym. Chem.*, 2017, **8**, 6534–6543.
26 P. K. Chattaraj, U. Sarkar and D. R. Roy, *Chem. Rev.*, 2006, **106**, 2065–2091.
27 L. G. Zhuo, W. Liao and Z. X. Yu, *Asian J. Org. Chem.*, 2012, **1**, 336–345.
28 R. G. Parr, L. V. Szentpály and S. Liu, *J. Am. Chem. Soc.*, 1999, **121**, 1922–1924.
29 R. Appel and H. Mayr, *J. Am. Chem. Soc.*, 2011, **133**, 8240–8251.
30 R. Lucius and H. Mayr, *Angew. Chem., Int. Ed.*, 2000, **39**, 1995–1997.
31 L. R. Domingo, M. J. Aurell, P. Pérez and R. Contreras, *J. Org. Chem.*, 2003, **68**, 3884–3890.
32 L. R. Domingo, M. J. Aurell, P. Pérez and R. Contreras, *J. Phys. Chem. A*, 2002, **106**, 6871–6875.
33 A. Corsaro, V. Pistarà, A. Rescifina, A. Piperno, M. A. Chiacchio and G. Romeo, *Tetrahedron*, 2004, **60**, 6443–6451.
34 H. Jangra, Q. Chen, E. Fuks, I. Zenz, P. Mayer, A. R. Ofial, H. Zipse and H. Mayr, *J. Am. Chem. Soc.*, 2018, **140**, 16758–16772.
35 Z. Li, H. Jangra, Q. Chen, P. Mayer, A. R. Ofial, H. Zipse and H. Mayr, *J. Am. Chem. Soc.*, 2018, **140**, 5500–5515.
36 R. Lonsdale, J. Burgess, N. Colclough, N. L. Davies, E. M. Lenz, A. L. Orton and R. A. Ward, *J. Chem. Inf. Model.*, 2017, **57**, 3124–3137.
37 D. S. Allgäuer, H. Jangra, H. Asahara, Z. Li, Q. Chen, H. Zipse, A. R. Ofial and H. Mayr, *J. Am. Chem. Soc.*, 2017, **139**, 13318–13329.
38 M. M. Kreevoy, E. T. Harper, R. E. Duvall, H. S. Wilgus and L. T. Ditsch, *J. Am. Chem. Soc.*, 1960, **82**, 4899–4902.
39 X. Han, R. Lee, T. Chen, J. Luo, Y. Lu and K.-W. Huang, *Sci. Rep.*, 2013, **3**, 2557.
40 K. J. Laidler and M. C. King, *J. Phys. Chem.*, 1983, **87**, 2657–2664.
41 K. Kim, N. R. Singstock, K. K. Childress, J. Sinha, A. M. Salazar, S. N. Whitfield, A. M. Holder, J. W. Stansbury and C. B. Musgrave, *J. Am. Chem. Soc.*, 2019, **141**, 6279–6291.
42 J. Sinha, M. Podgórski, S. Huang and C. N. Bowman, *Chem. Commun.*, 2018, **54**, 3034–3037.
43 H. S. Yu, X. He, S. L. Li and D. G. Truhlar, *Chem. Sci.*, 2016, **7**, 5032–5051.
44 M. J. Frisch, G. W. Trucks, H. B. Schlegel, G. E. Scuseria, M. A. Robb, J. R. Cheeseman, G. Scalmani, V. Barone, G. A. Petersson, H. Nakatsuji, X. Li, M. Caricato, A. V. Marenich, J. Bloino, B. G. Janesko, R. Gomperts, B. Mennucci, H. P. Hratchian, J. V. Ortiz, A. F. Izmaylov, J. L. Sonnenberg, D. Williams-Young, F. Ding, F. Lipparini, F. Egidi, J. Goings, B. Peng, A. Petrone, T. Henderson, D. Ranasinghe, V. G. Zakrzewski, J. Gao, N. Rega, G. Zheng, W. Liang, M. Hada, M. Ehara, K. Toyota, R. Fukuda, J. Hasegawa, M. Ishida, T. Nakajima, Y. Honda, O. Kitao, H. Nakai, T. Vreven, K. Throssell, J. A. Montgomery Jr., J. E. Peralta, F. Ogliaro, M. J. Bearpark, J. J. Heyd, E. N. Brothers, K. N. Kudin, V. N. Staroverov, T. A. Keith, R. Kobayashi, J. Normand, K. Raghavachari, A. P. Rendell, J. C. Burant, S. S. Iyengar, J. Tomasi, M. Cossi, J. M. Millam, M. Klene, C. Adamo, R. Cammi, J. W. Ochterski, R. L. Martin, K. Morokuma, O. Farkas, J. B. Foresman and D. J. Fox, *Gaussian 16, Revision A.03*, Gaussian, Inc., Wallingford CT, 2016.
45 A. V. Marenich, C. J. Cramer and D. G. Truhlar, *J. Phys. Chem. B*, 2009, **113**, 6378–6396.
46 M. D. Hanwell, D. E. Curtis, D. C. Lonie, T. Vandermeersch, E. Zurek and G. R. Hutchison, *J. Cheminf.*, 2012, **4**, 1–17.